IOPscience iopscience.iop.org

Home Search Collections Journals About Contact us My IOPscience

High-temperature thermoelectric performance of Si–Ge alloys

This article has been downloaded from IOPscience. Please scroll down to see the full text article.

2003 J. Phys.: Condens. Matter 15 5359

(http://iopscience.iop.org/0953-8984/15/31/303)

View the table of contents for this issue, or go to the journal homepage for more

Download details:
IP Address: 171.66.16.121
The article was downloaded on 19/05/2010 at 14:23

Please note that terms and conditions apply.

Institute of Physics Publishing — Journal of Physics: Condensed Matter

J. Phys.: Condens. Matter **15** (2003) 5359–5370 — PII: S0953-8984(03)60446-7

High-temperature thermoelectric performance of Si–Ge alloys

M N Tripathi[1] **and C M Bhandari**[2]

Department of Physics, University of Allahabad, Allahabad 211002, India

Received 3 March 2003
Published 23 July 2003
Online at stacks.iop.org/JPhysCM/15/5359

Abstract

A detailed study of the variation of the thermoelectric figure of merit of Si–Ge alloys with alloy composition, temperature and carrier density is the subject matter of this paper. Such a study is of particular interest at higher temperatures when minority carrier effects (MCEs) start to play a significant role in degrading the performance, thereby setting an upper limit of high temperature application. Alloys rich in silicon content are of greater interest and attention for the obvious reason that silicon, due to its large energy gap, is important in pushing the MCE to higher temperatures. The purpose of the present paper is to examine in depth all those processes that tend to degrade the material performance.

Thermoelectric materials are heavily doped and hence a single-band conduction model (conduction band in n-type, valence band in p-type) is quite a good choice at low and moderately high temperatures. However, with increasing temperature the applicability of single-band conduction becomes questionable. A two-band conduction model is then necessary. For single-band conduction the thermoelectric figure of merit (Goldsmid 1960, 1988, Rowe and Bhandari 1983, Rowe 1995) is given by

$$Z = \alpha^2\sigma/\lambda \tag{1}$$

where α, σ and λ refer to the Seebeck coefficient, electrical conductivity and thermal conductivity of the material, respectively.

Low thermal conductivity materials are a better choice as thermoelements for the obvious reason. For low doping levels this can be decided by the lattice contribution to thermal conductivity which is the dominant heat transport mechanism. However, in the heavily doped materials electronic (or hole) contribution to thermal transport could not be ignored. Electronic (hole) thermal conductivity in the heavily doped samples is essentially due to a single carrier type. However, at high temperatures one must take into account contributions from both the

[1] CMP Degree College, Allahabad, India.

[2] Present address: Indian Institute of Information Technology, Allahabad, India.

bands and also the bipolar contribution. The total thermal conductivity (Drabble and Goldsmid 1961, Bhandari and Rowe 1988, Slack and Hussain 1991, Rowe 1995) is then given as

$$\lambda = \lambda_L + \lambda_e + \lambda_h + \lambda_b \tag{2}$$

where subscripts L, e, h and b, respectively, refer to lattice, electron, hole and electron–hole pair (bipolar) contributions. On application of a temperature gradient electron–hole pairs flow down the temperature gradient transporting energy, but no net charge. A sharp rise in thermal conductivity due to these contributions may result in degradation of material performance.

Thermoelectric materials being heavily doped, the usual assumption of a parabolic energy band with a constant effective mass for carriers may not correspond to real situation. To get a reasonably accurate estimate of the system behaviour deviations from the strict parabolic band need to be taken into consideration. The present calculation incorporates the effect of non-parabolicity of energy bands by considering an electron (hole) effective mass (Ravich *et al* 1971, Goldsmid 1988) given by

$$m^* = m_0^*(1 + 2\beta_g \eta) \qquad \text{where } \beta_g = \frac{k_B T}{E_g} \text{ and } \eta = \frac{E}{k_B T}. \tag{3}$$

β_g and η refer respectively to the inverse of the reduced energy band gap and reduced carrier energy. m_0^* refers to the effective mass at the band edge.

A theoretical calculation of all the relevant properties requires information about the carrier relaxation time which may be determined by various scattering mechanisms. At the temperatures of interest in the present work (600–1600 K) acoustic phonon scattering is the dominant mechanism and is largely responsible for limiting the carrier mean free path. In a many-valley semiconductor such as the Si–Ge alloy system both inter- and intra-valley scattering of carriers must be taken into account. This should be particularly so for higher temperature calculations. However, in view of too many complications arising out of the non-parabolic nature of energy bands, several equivalent valleys and minority carrier effects (MCEs), we have currently restricted ourselves to only intra-valley scattering.

The corresponding relaxation time (Smirnov and Ravich 1967, Ravich *et al* 1971), which takes account of the non-parabolicity of the energy bands, is given by

$$\tau_{ac}^{-1} \propto [\eta(1 + \beta_g \eta)]^{\frac{1}{2}}[1 + 2\beta_g \eta]. \tag{4}$$

For non-parabolic energy bands the transport coefficients can be expressed in terms of generalized Fermi integrals (Smirnov and Ravich 1967, Ravich *et al* 1971, Rowe and Bhandari 1985, Rowe 1995) defined by

$${}^nL_l^m(\xi, \beta_g) = \int_0^\infty \left(-\frac{\partial f}{\partial \eta}\right)\eta^n[\eta(1 + \beta_g\eta)]^m(1 + 2\beta_g\eta)^l \, d\eta. \tag{5}$$

Here f is the Fermi distribution function and $\xi = (E_F)/(k_B T)$ refers to reduced Fermi energy. The indices n, m and l take different values for various scattering processes.

The reduced electrical conductivity σ' is given by

$$\sigma' = \left(\frac{k_B}{e}\right)^2 \frac{T}{\lambda_l}\sigma = K N_V \, {}^0L_{-2}^1 \frac{T}{[m_c^* \lambda_l]} \tag{6}$$

where N_V is the number of equivalent valleys and m_c^* is the conductivity effective mass. In the present calculations no distinction has been made between the density-of-states and conductivity effective masses. The constant K depends on the elastic constant C_{11} and acoustic deformation potential (ξ_D) and is given by Drabble and Goldsmid (1961), Bhandari and Rowe (1988), Rowe (1995)

$$K = \frac{k_B^2 h C_{11}}{3\pi^2 \xi_D^2}. \tag{7}$$

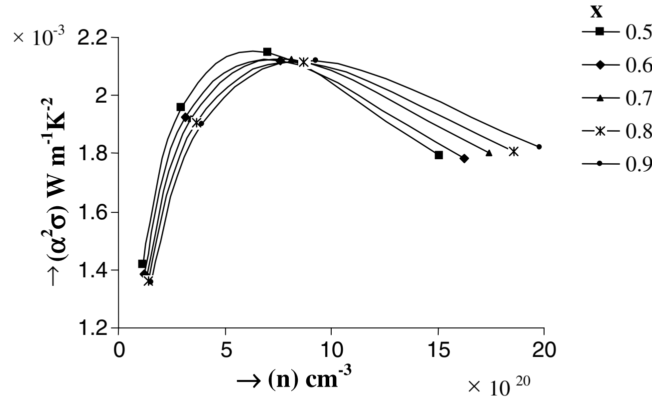

Figure 1. Variation of power factor ($\alpha^2\sigma$) with carrier density (n) at temperature 1000 K for different alloy compositions of $\mathrm{Si}_x\mathrm{Ge}_{(1-x)}$.

The contribution to the Seebeck coefficient from the jth band can be expressed as

$$\alpha_j = \frac{k_B}{e}\left[\frac{{}^1L^1_{-2}}{{}^0L^1_{-2}} - \xi_j\right]. \tag{8}$$

In two-band conduction the electrical conductivity is the sum of contributions from both electron and hole bands. The total Seebeck coefficient (Rowe and Bhandari 1985, Rowe 1995) is given by

$$\alpha = [\alpha_e\sigma_e + \alpha_h\sigma_h]/(\sigma_e + \sigma_h). \tag{9}$$

Increased electrical conductivity for higher doping levels will also be accompanied by an increased electron (hole) contribution to the thermal transport which now becomes significant and needs to be taken care of. The electronic contribution to the thermal conductivity is given by

$$\lambda_e = K N_V\, {}^0L^1_{-2}\frac{T}{m_c^*}\left(\frac{{}^2L^1_{-2}}{{}^0L^1_{-2}} - \left[\frac{{}^1L^1_{-2}}{{}^0L^1_{-2}}\right]^2\right). \tag{10}$$

Equations (6) and (10) help us in determining the Lorenz number defined as

$$L_{e,h} = \frac{\lambda_{e,h}}{\sigma T}. \tag{11}$$

Thermoelectric figure of merit

For two-band conduction the reduced figure of merit (Ure 1972, Rowe 1995) is given by

$$(ZT)'_{2B} = \frac{(\alpha'_h\sigma'_h - \alpha'_e\sigma'_e)^2}{(\sigma'_e + \sigma'_h)(1 + L_e\sigma'_e + L_h\sigma'_h)}. \tag{12}$$

Here α'_e and α'_h refer to reduced Seebeck coefficients defined by $\alpha'_{e,h} = (e/k_B)\alpha_{e,h}$. This expression excludes a bipolar contribution to thermal conduction. In the intrinsic region, a sufficient number of electron–hole pairs are created, which conduct heat but not electric charge. Including the bipolar contribution to the thermal conductivity the figure of merit (Goldsmid 1960, Ure 1972, Rowe and Bhandari 1985, Rowe 1995) becomes

$$ZT = \frac{(\alpha'_h\sigma'_h - \alpha'_e\sigma'_e)^2}{\{(\sigma'_e + \sigma'_h)(1 + \sigma'_e L_e + \sigma'_h L_h) + \sigma'_e\sigma'_h(\delta_e + \delta_h + \xi_g)^2\}} \tag{13}$$

where $\delta = {}^1L^1_{-2}/{}^0L^1_{-2}$ and $\xi_g = E_g/k_BT$.

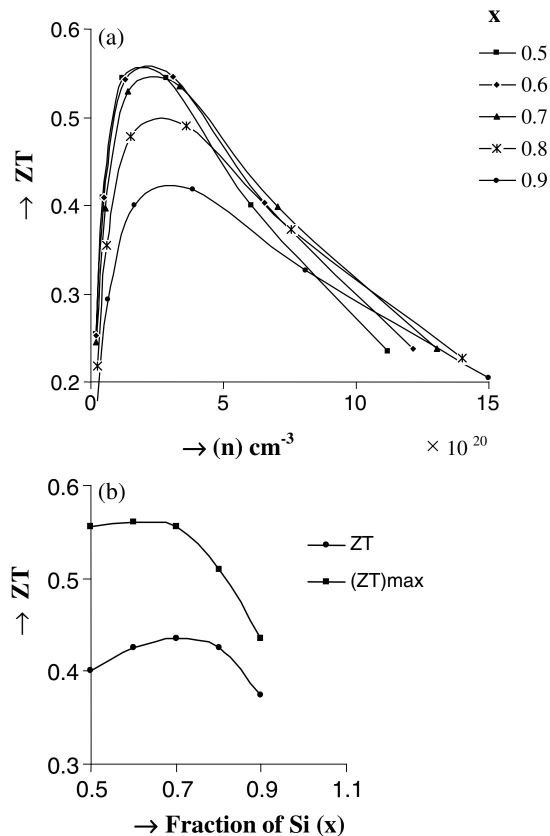

Figure 2. (a) Variation of figure of merit (ZT) with n at 600 K for different alloy compositions of $Si_xGe_{(1-x)}$. (b) Variation of figure of merit (ZT) for fixed $n = 6 \times 10^{20}$ cm^{-3} and $(ZT)_{max}$ with different alloy compositions at 600 K.

Optimization of material performance

All thermoelectric optimization programmes take up independently varying parameters and then look into the combination of such parameters which may yield the highest figure of merit. For theoretical models it is very useful to consider reduced Fermi energy as an independent variable and vary it over a wide range—from the nondegenerate to the degenerate range. However, physical realization of this includes samples which are undoped on the one hand to samples which are doped to saturation. To assume a particular scattering type, such as acoustic phonon scattering, may not be true in general for the entire range. However, the temperature range of interest in the present context is such that this assumption would not create a serious error as all donor states are already ionized. However, exclusion of intervalley scattering is not wholly justified, and should be taken care of in an extended version of the work.

In addition to ξ (reduced Fermi energy), alloy composition (percentage silicon content x) has been varied for $x \geqslant 0.5$. Energy bandgap is known to vary almost linearly in the range of composition. We have assumed a similar scheme of interpolation for elastic constants, effective mass and deformation potential.

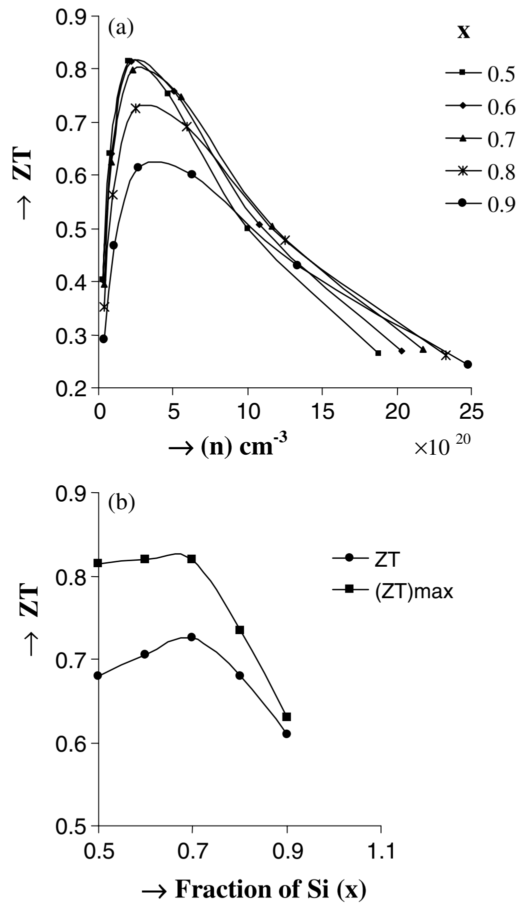

Figure 3. (a) Variation of figure of merit (ZT) with n at 800 K for different alloy compositions. (b) Variation of figure of merit (ZT) for fixed $n = 6 \times 10^{20}$ cm^{-3} and $(ZT)_{\max}$ with different alloy compositions at 800 K.

Lattice thermal conductivity

Alloying has a strong influence on lattice thermal conductivity (Dismukes *et al* 1964). It is partly due to a sizeable reduction in λ_L due to alloy disorder scattering of phonons that alloys are automatically a better choice than the pure constituents. The reduction in λ_L may be of an order of magnitude. Lattice thermal conductivity of Si–Ge alloys has been studied in detail (Drabble and Goldsmid 1961, Dismukes *et al* 1964, Bhandari and Rowe 1988) in the framework of the relaxation time approximation. Only a brief outline is being given here. Assuming the addition of inverse relaxation times for various phonon scattering processes $\tau_C^{-1} = \sum_i \tau_i^{-1}$ (τ_i being the relaxation time for the particular scattering mechanism), the lattice thermal conductivity is given by Drabble and Goldsmid (1961), Bhandari and Rowe (1988)

$$\lambda_L = \left(\frac{k_B}{\hbar}\right)^3 \frac{k_B}{2\pi^2 v_s} T^3 \int_0^{\theta_D/T} \frac{x^4 e^4}{(e^x - 1)^2} \tau_C \, dx. \quad (14)$$

Here θ_D is the Debye temperature.

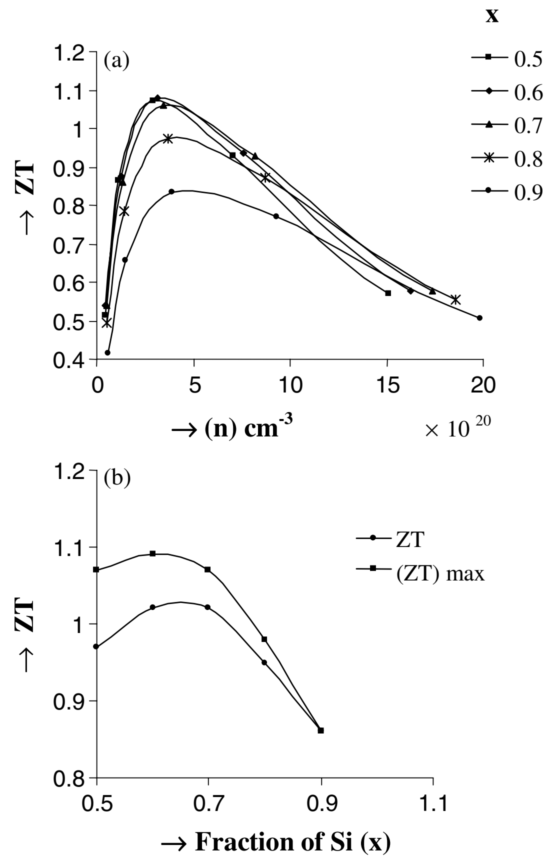

Figure 4. (a) Variation of figure of merit (ZT) with n at 1000 K for different alloy compositions of $\mathrm{Si}_x\mathrm{Ge}_{(1-x)}$. (b) Variation of figure of merit (ZT) for fixed $n = 6 \times 10^{20}$ cm^{-3} and $(ZT)_{\max}$ with different alloy compositions at 1000 K.

The main scattering agents that limit the phonon mean free path are scattering by phonons and alloy disorder. Variation in lattice thermal conductivity of the alloys with composition is due to disorder scattering; the phonon relaxation time for alloy disorder scattering can be expressed in a simple form

$$\tau^{-1}_{\mathrm{ph(disorder)}} = \frac{\Gamma\omega^2 g(\omega)}{6N}. \tag{15}$$

Here ω is the phonon frequency, N is the number of atoms in a crystal of volume V. Γ, which is a measure of the strength of mass-difference scattering, is given by

$$\Gamma = \sum_i f_i\left(1 - \frac{M_i}{\bar{M}}\right)^2, \tag{16}$$

f_i is the fractional concentration of the ith type of atoms of mass M_i and $\bar{M} = \sum_i f_i M_i$ is the average atomic mass. For the Debye model phonon density of states $g(\omega) = 3V\omega^2/2\pi^2 v_s^3$. Here V is the crystal volume and v_s is the average phonon velocity.

Further reduction in λ_L could be achieved by using powder compacts. Fine-grained Si–Ge alloys have been earlier studied with reference to thermal conductivity reductions (Bhandari and

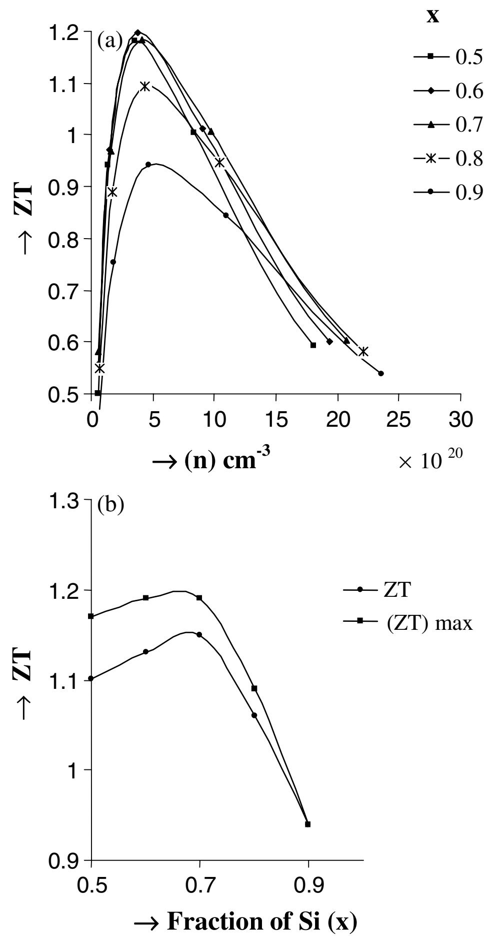

Figure 5. (a) Variation of figure of merit (ZT) with n at 1100 K for different alloy compositions. (b) Variation of figure of merit (ZT) for fixed $n = 6 \times 10^{20}$ cm^{-3} and $(ZT)_{max}$ with different alloy compositions at 1100 K.

Table 1. Physical parameters of Si and Ge used in the calculations.

	E_g (eV)	m_d^*/m_0	C_{11} (10^{11} N m^{-2})	ξ_D (eV)	λ_L (W m^{-1} K^{-1})	N_V
Silicon	1.15	1.06	1.66	12.8	150	6
Germanium	0.65	0.56	1.28	12.9	58	4

Rowe 1978a, 1978b). Up to a critical grain size electronic (hole) mean free path is not affected, thereby causing an increased value of electrical to thermal conductivity ratio (Bhandari and Rowe 1980).

Various physical parameters pertaining to the Si–Ge system are displayed in table 1.

For different alloy compositions λ_L has been obtained from alloy disorder scattering formulae, equations (14)–(16). For other parameters such as E_g, m_d, C_{11} and ξ_D a linear interpolation has been considered.

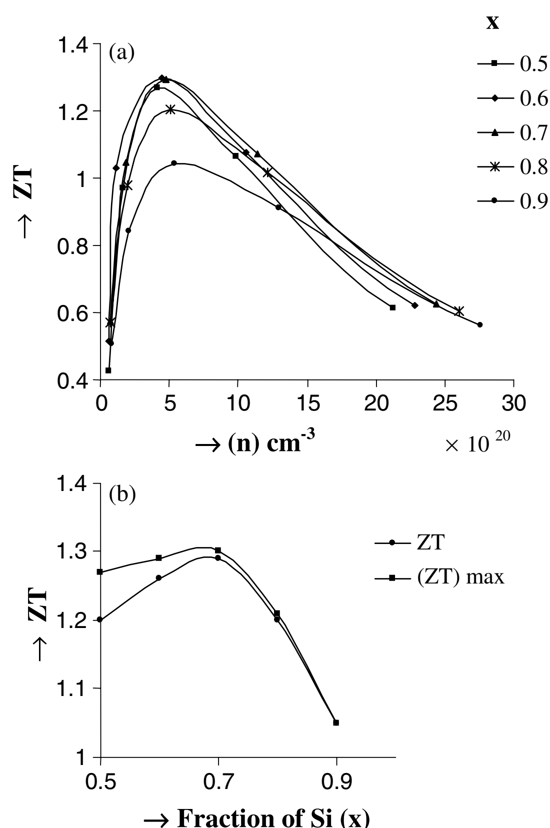

Figure 6. (a) Variation of figure of merit (ZT) with n at 1200 K for different alloy compositions of $Si_xGe_{(1-x)}$. (b) Variation of figure of merit (ZT) for fixed $n = 6 \times 10^{20}$ cm^{-3} and $(ZT)_{max}$ with different alloy compositions at 1200 K.

Results and discussion

A detailed calculation of power factor and dimensionless thermoelectric figure of merit ZT has been presented as a function of carrier density (n), alloy composition (% silicon content, x) and temperature. In figure 1 we present the power factor ($\alpha^2\sigma$) plotted against (n) at 1000 K for x ranging from 0.5 to 0.9. This figure is representative of variation of power factor at other temperatures also. Optimal carrier density for various temperatures ranges from 2×10^{20} to 8×10^{20} cm^{-3}. However, our primary aim is to obtain a realistic estimate of thermoelectric figure of merit (ZT) in a wide temperature range. Any difference between these alloys' thermoelectric behaviour is reflected better in ZT, obviously due to significant differences in λ_L. Figure 2(a) displays variation of ZT with carrier density at 600 K for various alloy compositions. Figure 2(b) shows ZT against alloy composition for fixed $n = 6 \times 10^{20}$ cm^{-3} and $(ZT)_{max,}$ which is the peak value of ZT for a given temperature. Similar plots for the alloy system at 800, 1000, 1100 and 1200 K are presented in figures 3(a) and (b), 4(a) and (b), 5(a) and (b) and 6(a) and (b). Figures 7(a) and (b) display the variation of ZT with temperature and alloy composition for two carrier concentrations. Thermoelectric devices operate over a temperature range between temperatures of the hot and cold junctions. Theoretically each temperature will have an optimum value for carrier density and alloy composition. However,

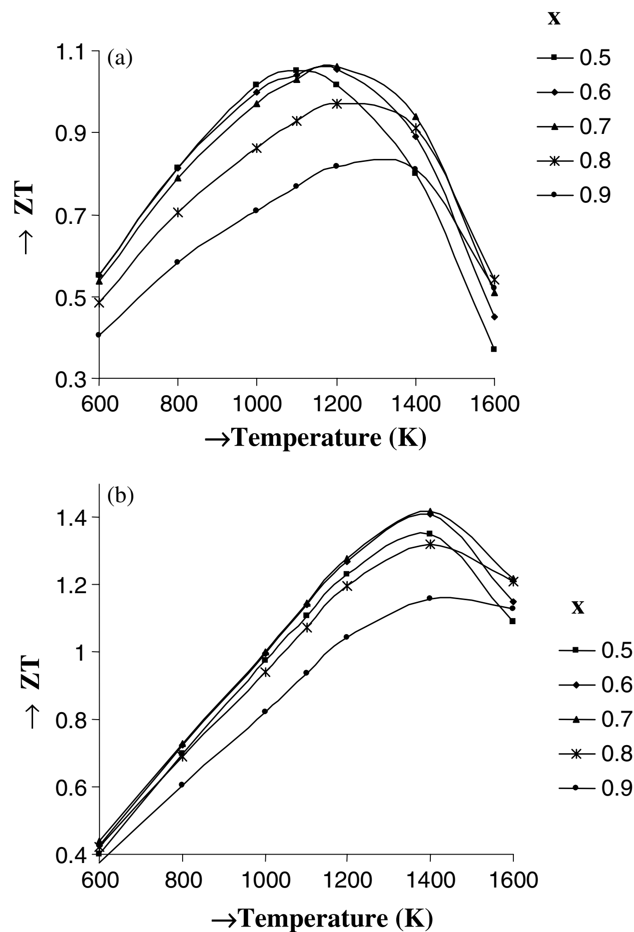

Figure 7. (a) Variation of figure of merit (ZT) with temperature (T) at fixed $n = 2 \times 10^{20}$ cm^{-3} for different alloy compositions. (b) Variation of figure of merit (ZT) with temperature (T) at fixed $n = 6 \times 10^{20}$ cm^{-3} for different alloy compositions.

this is not possible to achieve in device fabrication and therefore the best possible choice has to be made. An alternative approach would be to consider cascading (Rowe and Bhandari 1983) which can help in choosing a different set of material parameters for each step. The information based on such a study can be of help in choosing optimum values for material parameters for various stages.

Figure 8 shows variation of ZT with x for temperatures above 1000 K at fixed $n = 6 \times 10^{20}$ cm^{-3}. These results show that x ranging between 0.65 and 0.70 appears to be ideally suited for best thermoelectric performance at temperatures exceeding 1000 K. Si–Ge alloys are not among the best known materials at lower temperatures. However, at higher temperatures (beyond 1000 K), these alloys provide a good choice for thermoelement material. Results of present calculations indicate a range for x $(0.5 < x < 0.7)$ for temperature range $600 < T < 1400$ K. At 1600 K the optimum may increase to 0.8; this is expected as at higher temperatures MCE can be countered by a larger energy gap.

It is also of interest to estimate the percentage reduction in ZT due to MCE. We have calculated ZT in both single-band and two-band models and obtained the percentage change

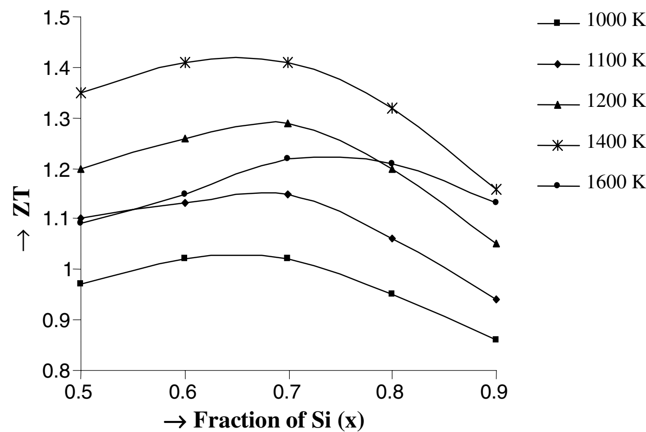

Figure 8. Variation of figure of merit (ZT) for (near optimal) $n = 6 \times 10^{20}$ cm^{-3} with fraction of silicon (x) in alloy composition at different temperatures.

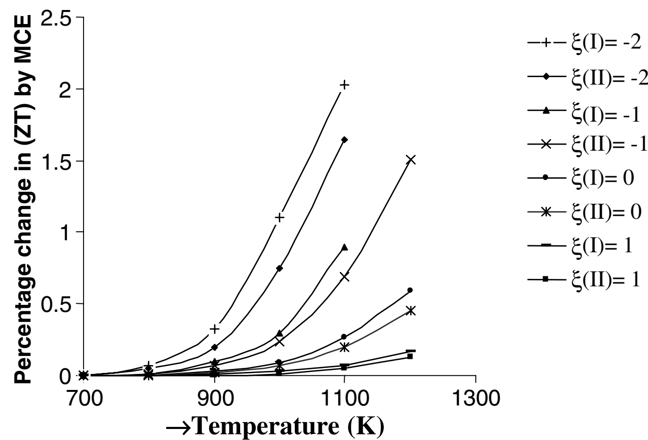

Figure 9. Variation of percentage change in ZT with temperature at different Fermi levels, considering both MCEs. Curves marked (I) indicate minority effects without bipolar thermal conductivity and curves (II) indicate all contributions.

in ZT as we go from one model to another. Obviously this change is expected to rise with (a) rising temperature, and (b) with lower carrier densities. Figure 9 displays such a variation of $\Delta(ZT)$ with temperature and reduced Fermi level for $x = 0.7$. The two curves for each ξ indicate the effect of different types of MCE. Curves marked (I) indicate minority effects without bipolar thermal conductivity (equation (12)) and curves (II) indicate all contributions (equation (13)). This shows the significant presence of bipolar heat transport at temperatures exceeding 1000 K. The results suggest the necessity of heavy doping to thwart dominance of MCE to the extent possible.

In order that the figure of merit of the doped alloys be optimized, it is necessary to dope Si–Ge alloys up to dopant concentrations at the solid solubility limits. In heavily doped materials dopant precipitation (Raag 1978, Rowe and Bhandari 1983) has been reported resulting in a change in electrical and thermoelectric properties. Hence the value of n appropriate for consideration could be decided on the basis of two competing factors: (a) dopant precipitation,

and (b) MCE (Rowe 1988). Larger n would increase precipitation whereas it will decrease MCE. On the other hand a low value of carrier density (n) may result in low precipitation but relatively high MCE. A proper balance between two factors may decide the optimum doping level.

There have been suggestions that gallium phosphide added to the Si–Ge alloy system could markedly increase the solid solubility (Wood 1988, Rowe *et al* 1989). It is not possible to include such effects in the present work. However, if such a possibility exists larger doping levels without the risk of significant precipitation could go a long way in enhancing performance of the Si–Ge system up to around 1400 K without risk of performance degradation either due to dopant precipitation, or due to MCE.

Recently Gurevich *et al* (1995, 2002) have presented a new approach to thermoelectric phenomena which deals with thermo-emf in bipolar semiconductors. The theory takes into account non-equilibrium distribution of electron and hole concentrations. Electron and hole electric conductances of the contacts (between sample and connecting wires) may make a substantial contribution to thermo-emf. However, as the authors themselves point out determination of these conductances may be quite a difficult task (Gurevich *et al* 1995). In addition to this, bulk and surface recombination of electrons and holes has been shown to be crucial in thermoelectric effects (Gurevich 1997). In bipolar semiconductors both electrons and holes diffuse down the temperature gradient, thereby increasing the electron and hole concentrations near the cold junction. In this situation the usual relation $np = n_i^2$ (where n and p are electron and hole equilibrium concentrations and n_i is the intrinsic concentration) may not be applicable. The correctness of this relation is based on the existence of common Fermi levels for electrons and holes. However, in this situation the common Fermi level is split into two Fermi quasi-levels. These aspects of non-equilibrium distribution and the recombination processes could form the basis of a more rigorous future approach in the study of thermoelectric phenomena.

Acknowledgments

The authors are thankful to Professor G K Pandey and Dr M D Tiwari for their interest and support. MNT thanks the Council of Scientific and Industrial Research, India for financial assistance and Suneet Dwivedi for suggestions and support.

References

Bhandari C M and Rowe D M 1978a *J. Phys. C: Solid State Phys.* **11** 1787

Bhandari C M and Rowe D M 1978b *Proc. 2nd Int. Conf. on Thermoelectric Energy Conversion (Arlington, TX, March 1978)* p 32

Bhandari C M and Rowe D M 1980 *Contemp. Phys.* **21** 219

Bhandari C M and Rowe D M 1988 *Thermal Conduction in Semiconductors* (New Delhi: Wiley)

Dismukes J P, Ekstrom L, Steigmeier E F, Kudman J and Beers D S 1964 *J. Appl. Phys.* **35** 2899

Drabble J R and Goldsmid H J 1961 *Thermal Conduction in Semiconductors* (Oxford: Pergamon)

Goldsmid H J 1960 *Applications of Thermoelectricity* (London: Methuen Monograph)

Goldsmid H J 1988 *Electronic Refrigeration* (London: Pion)

Gurevich Yu G 1997 *J. Thermoelectricity* **2** 5

Gurevich Yu G, Logvinov G N, Volovichev I N, Espejo G, Titov O Yu and Meriuts A 2002 *Phys. Status Solidi* b **231** 278

Gurevich Yu G, Titov O Yu, Logvinov G N and Lyubimov O I 1995 *Phys. Rev.* B **51** 6999

Raag V 1978 *Proc. 2nd Int. Conf. on Thermoelectric Energy Conversion (Arlington, TX, March 1978)* p 5

Ravich Y I, Efimova B A and Tamarchenko V I 1971 *Phys. Status Solidi* b **43** 11

Rowe D M 1988 *1st Eur. Conf. on Thermoelectrics* (London: Peregrinus) p 178

Rowe D M 1995 *CRC Handbook of Thermoelectrics* (Boca Raton, FL: Chemical Rubber Company Press)
Rowe D M and Bhandari C M 1983 *Modern Thermoelectrics* (London: Holt Saunders)
Rowe D M and Bhandari C M 1985 *J. Phys. D: Appl. Phys.* **18** 873
Rowe D M, Min G and Bhandari C M 1989 *Proc. 2nd Asian Thermophysical Properties Conf.* p 145
Slack G A and Hussain M A 1991 *J. Appl. Phys.* **70** (5) 2694
Smirnov I A and Ravich Y I 1967 *Sov. Phys.–Semicond.* **1** 739
Ure R W Jr 1972 *Energy Convers.* **12** 45
Wood C 1988 *1st Eur. Conf. on Thermoelectrics* (London: Peregrinus) p 1